FEBS Letters 587 (2013) 3437–3443

FEBS Letters

journal homepage: www.FEBSLetters.org

γH2AX foci formation in the absence of DNA damage: Mitotic H2AX phosphorylation is mediated by the DNA-PKcs/CHK2 pathway

Wen-Zhi Tu [a,b,1], Bing Li [b,1], Bo Huang [a], Yu Wang [b], Xiao-Dan Liu [b], Hua Guan [b], Shi-Meng Zhang [b], Yan Tang [a], Wei-Qing Rang [a,*], Ping-Kun Zhou [a,b,*]

[a] Institute for Environmental Medicine and Radiation Hygiene, The College of Public Health, University of South China, Hengyang, Hunan Province 421000, PR China
[b] Department of Radiation Toxicology and Oncology, Beijing Institute of Radiation Medicine, Beijing 100850, PR China

ARTICLE INFO

Article history:
Received 11 June 2013
Revised 6 August 2013
Accepted 21 August 2013
Available online 8 September 2013

Edited by Varda Rotter

Keywords:
γH2AX
CHK2
DNA-PKcs
DNA damage
Mitosis

ABSTRACT

Phosphorylated H2AX is considered to be a biomarker for DNA double-strand breaks (DSB), but recent evidence suggests that γH2AX does not always indicate the presence of DSB. Here we demonstrate the bimodal dynamic of H2AX phosphorylation induced by ionizing radiation, with the second peak appearing when G2/M arrest is induced. An increased level of γH2AX occurred in mitotic cells, and this increase was attenuated by DNA-PKcs inactivation or *Chk2* depletion, but not by ATM inhibition. The phosphorylation-mimic CHK2-T68D abrogated the attenuation of mitotic γH2AX induced by DNA-PKcs inactivation. Thus, the DNA-PKcs/CHK2 pathway mediates the mitotic phosphorylation of H2AX in the absence of DNA damage.

1. Introduction

DNA double-strand breaks (DSBs) are the most dangerous type of DNA damage, as even a single unrepaired DSB can result in cell death [1,2]. DSBs can be repaired through the homologous recombination (HR) or non-homologous end joining (NHEJ) pathways [1,3]. One of the earliest events in the cellular response to DSBs is the phosphorylation of H2AX at Ser139, which is referred to as γH2AX [4]. H2AX is a member of the histone protein H2A family; the other two members are H2A1-H2A2 and H2AZ [5]. γH2AX foci formation at DSB sites occurs rapidly (within minutes) and is highly conserved from yeast to humans [6]. γH2AX can recruit other DSB signaling and repair factors such as MDC1, 53BP1 and the MRN complex to the damage site, forming nuclear ionizing radiation-induced foci (IRIF) [7–9]. Silencing H2AX increases radiosensitivity and interferes with the recruitment of DNA damage response proteins to the damage sites [10].

The phosphorylation of H2AX in response to DSBs is mediated by PIKK family proteins, which are characterized by the SQ/TQ motif. The members of the PIKK family include ataxia telangiectasia mutated (ATM), ataxia telangiectasia and rad3 related (ATR) and DNA dependent protein kinase catalytic subunit (DNA-PKcs). ATM and DNA-PKcs participate in the DSB signaling cascade, and both have been reported to phosphorylate H2AX [11,12]. ATR phosphorylates H2AX during replication fork blockage induced by UV exposure [13]. Thus, all of the PIKK family members contribute to the phosphorylation of H2AX in response to DSBs induced by ionizing radiation [14]. Although ATM is considered to be the major kinase responsible for H2AX phosphorylation during the DSB response, the recruitment and activation of ATM itself requires γH2AX [15], which could partially explain how γH2AX contributes to cell cycle arrest in response to DNA damage [16].

Due to the fact that γH2AX appears early and forms foci at damage sites, it is widely considered to be a sensitive biomarker for IR-induced DSBs [17]. However, γH2AX does not always indicate the presence of DSBs, and there is increasing evidence that calls into question the interpretation of γH2AX involvement in DSBs [18]. For instance, H2AX phosphorylation is also induced by UV radiation [18,19]. Serum starvation, which does not cause DNA damage, can induce the phosphorylation of H2AX through the p38 MAPK signaling pathway, which is closely associated with the induction of apoptosis [20]. Moreover, H2AX can be phosphorylated in

* Corresponding authors. Address: Institute for Environmental Medicine and Radiation Hygiene, The College of Public Health, University of South China, 28 Changsheng West-Road, Hengyang, Hunan Province 421000, PR China. (W.-Q. Rang). Address: Department of Radiation Toxicology and Oncology, Beijing Institute of Radiation Medicine, 27 Taiping Road, Beijing 100850, PR China. Fax: +86 10 68183899 (P.-K. Zhou).

E-mail addresses: nhurwq@126.com (W.-Q. Rang), zhoupk@bmi.ac.cn (P.-K. Zhou).

[1] These authors contributed equally to this work.

0014-5793/$36.00 © 2013 Federation of European Biochemical Societies. Published by Elsevier B.V. All rights reserved.
http://dx.doi.org/10.1016/j.febslet.2013.08.028

mitotic cells in the absence of DNA damage [11,21], and forms nuclear foci that do not recruit DNA damage response proteins [21]. This cell cycle-specific phosphorylation of H2AX suggests that a decrease in γH2AX levels may not accurately reflect DSB repair efficiency, because DSBs induce cell cycle arrest. However, little is known about the regulation of γH2AX in association with cell cycle progression.

The goal of the present study was to increase our understanding of mitotic H2AX phosphorylation. We found that DNA-PKcs, but not ATM, is responsible for the mitotic phosphorylation of H2AX in the absence of DNA damage, and that the cell cycle checkpoint protein 2 (CHK2) directly mediates this process. CHK2 was phosphorylated in a DNA-PKcs-dependent manner and was essential for H2AX phosphorylation. Our results show that the DNA-PKcs/Chk2 pathway is involved in mitotic H2AX phosphorylation.

2. Materials and methods

2.1. Cell culture

HeLa cells were maintained in DMEM (HyClone) supplemented with 10% fetal bovine serum (HyClone). HeLa cell lines overexpressing CHK2 were generated by transfecting with HeLa cells with wild-type and mutated *chk*2-expressing vectors. Meanwhile, a *Chk*2 knock-down HeLa cell line was generated by transfecting HeLa cells with a *chk*2 shRNA-expressing vector and selecting with Hygromycin B. To arrest cells in mitosis, 100 ng/ml nocodazole (M1404-2MG, Sigma) was added to the cell culture medium for 16 h. The cells were treated with 10 μM NU7026 (N1537, Sigma) or 10 μM KU55933 (S1092, Selleck) for 2 h to inhibit the PIKK activity of DNA-PKcs and ATM, respectively.

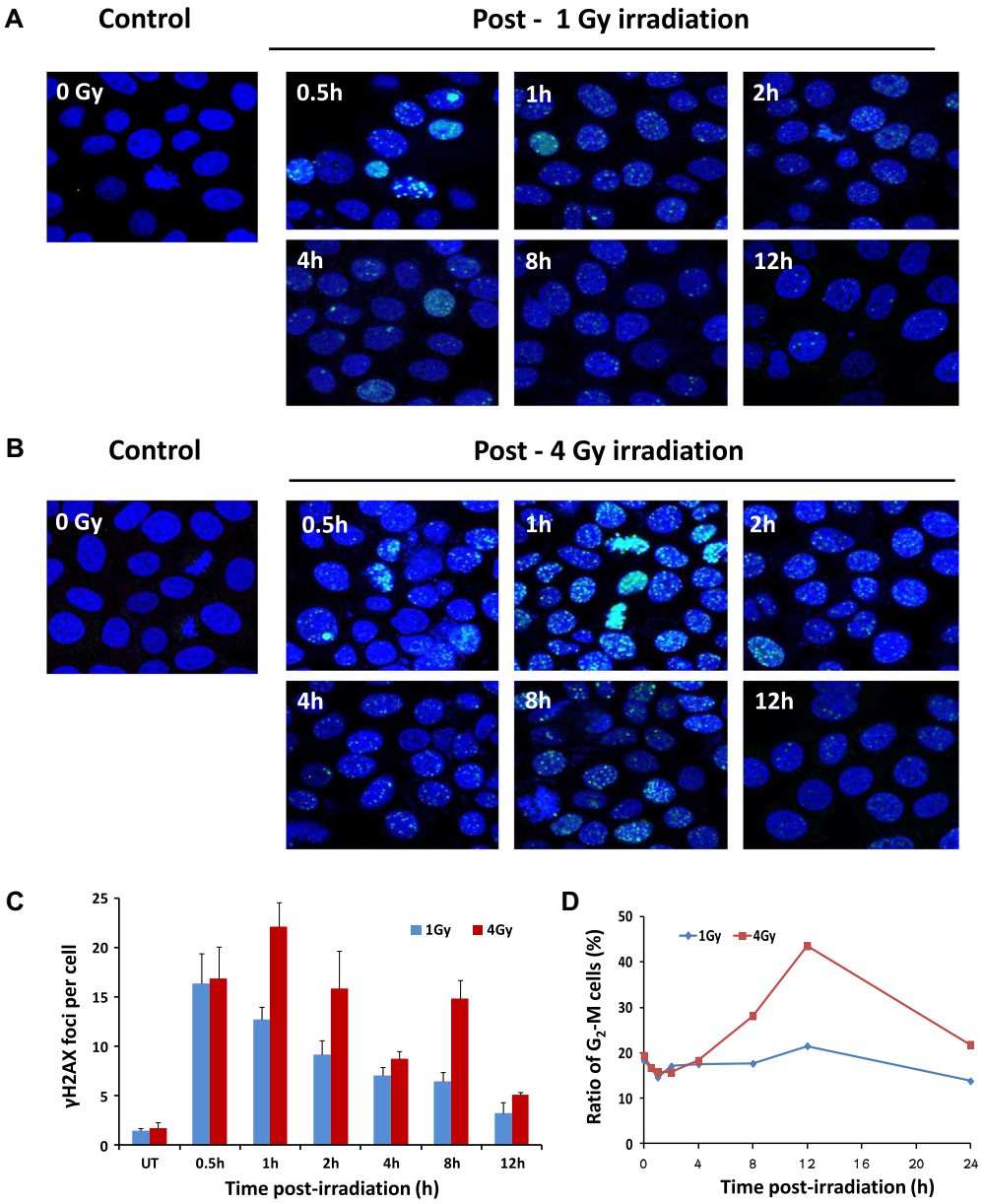

Fig. 1. Bimodal pattern of H2AX phosphorylation after treatment with a high dose of ionizing radiation. (A, B) γH2AX foci in HeLa cells after irradiation with 1 Gy (A) or 4 Gy (B) γ-rays. The cells were collected and fixed at the indicated time points after irradiation. (C) The dynamics of γH2AX foci formation after irradiation as shown in (A) & (B). Data are presented as mean ± S.D. from three independent experiments. (D) The proportion of of G2/M cells after treatment with 1 Gy or 4 Gy of irradiation, as measured by flow cytometric analysis.

2.2. Antibodies and immunoblotting

The antibodies against DNA-PKcs (H-163, sc-9051), PLK1 (E-2, sc-55504), CCNB1 (GNS1, sc-245), Ku80 (H-300, sc-9034), and β-actin (C4, sc-47778) were purchased from Santa Cruz Biotechnology. The antibodies against p-Chk2-T68 (C13C1, #2197) and CHK2 (#2662) were purchased from Cell Signaling Technology. The γH2AX (Ser 139) (JBW301, #05-636) antibody was purchased from Millipore. The DNA-PKcs p2056 (ab18192) antibody was purchased from Abcam.

For the immunoblotting (western blotting) analyses, the cells pellets were treated with lysis buffer, and the total protein was isolated. The proteins (50 μg) were resolved by SDS–PAGE and then transferred to a nitrocellulose (NC) membrane for immunoblotting analysis.

2.3. Microscopy imaging of immunofluorescence staining

The cells were grown on poly-D-lysine-coated culture slides (BD Pharmingen), washed in PBS, fixed in 4% paraformaldehyde/PBS for 30 min, permeabilized in 0.5% Triton X-100/PBS for 15 min, and blocked in blocking buffer (1% bovine serum albumin in PBS) for 30 min, as described previously [22]. Immunostaining was performed using an anti-γH2AX antibody for 2 h at room temperature in a humidified chamber. After three 10 min washes, the cells were incubated with the secondary antibody. The DNA was stained using a mounting medium with 4′,6-diamidino-2-phenylindole (DAPI, Sigma). Confocal immunofluorescence microscopy imaging was performed using an LSM 510 laser-scanning confocal microscope (Zeiss). The γH2AX foci were counted. Three independent experiments were performed.

2.4. Flow cytometric analysis of the cell cycle

The detailed protocol is described in the online Supplemental data.

2.5. shRNA, plasmid construction and transfection

The shRNA oligonucleotide targeting *Chk2* (5′-GAACCUGAG GACCAAGAAC-3′) was synthesized as described previously [23] and inserted into the BamHI and BbsI sites of the pGPU6/Hygro expression vector (GenePharma). For the negative control, a nonsense shRNA sequence was purchased from GenePharma (5′-TTCTCCGAACGTGTCACGT-3′). All construct sequences were verified before use. The wild-type and mutated *Chk2* plasmids and transfection methods are described in the online Supplemental data.

3. Results

3.1. Bimodal dynamics of H2AX phosphorylation in cells exposed to a high dose of ionizing radiation

To investigate the dynamics of H2AX phosphorylation post-ionizing radiation (IR), HeLa cells were irradiated with 1 Gy (low dose) or 4 Gy (high dose). As shown in Fig. 1(A,C), the number of γH2AX foci reached a peak at 30 min post-IR and then decreased gradually in cells exposed to 1 Gy (low dose). When the cells were irradiated with 4 Gy (high dose), the number of γH2AX foci reached a peak at 1 h and then declined. However, a second peak appeared at about 8 h post-IR in the cells irradiated with 4 Gy (Fig. 1B, C). Neutral single cell gel electrophoresis demonstrated that the DNA DSBs had

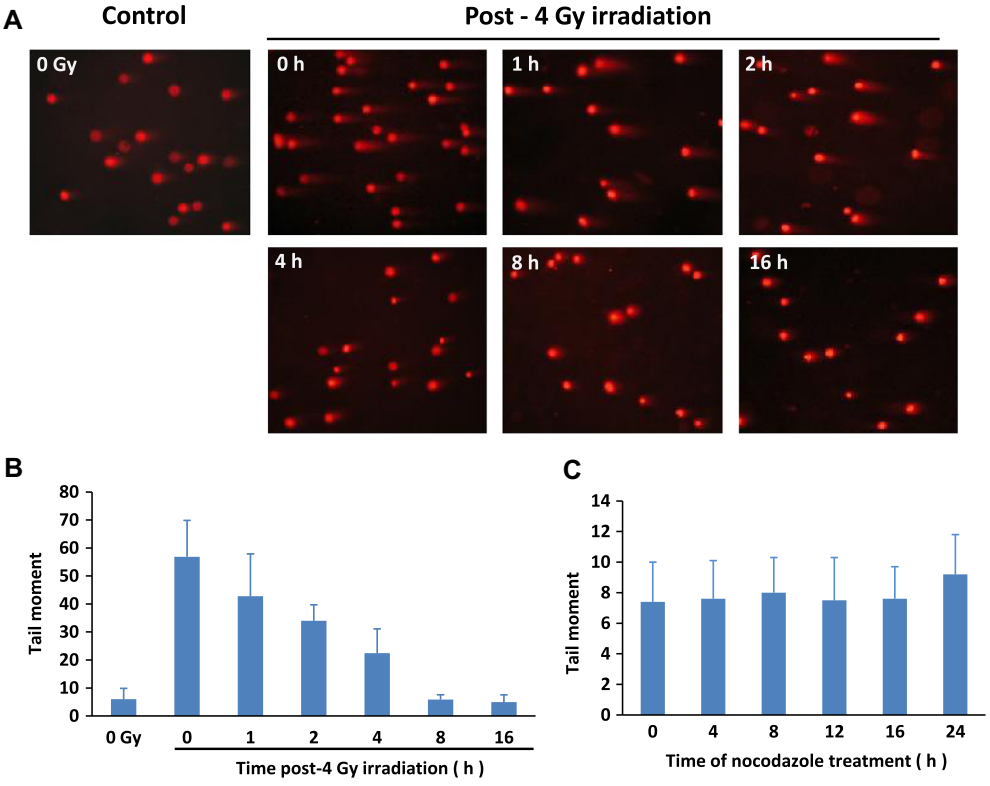

Fig. 2. Detection of DNA double-strand breaks (DSB) by neutral gel electrophoresis (comet) assay. (A) The comet images of HeLa cells at given times after 4 Gy irradiation or unirradiated control. (B) The repair kinetics of 4 Gy-induced DNA DSBs, which were expressed as the comets Olive tail moments. The data are the means and standard deviation from three experiments, and more than 50 comets were analyzed in each experiment. (C) The yield of DNA DSBs were detected by comet assay in HeLa cells at different times of treatment with 100 ng/ml nocodazole. The data (Olive tail moments) are the means and standard deviation from three experiments.

almost completely been repaired at 8 h post-IR (Fig. 2A, B). Therefore, the second γH2AX peak was most likely attributable to some other cellular response to IR other than DSBs. Flow cytometric analysis clearly showed the induction of G2/M mitotic arrest 8 h after the administration of 4 Gy of irradiation (Fig. 1D), while very few cells were arrested in the G2/M phase in the 1 Gy-irradiated cells. Therefore, we hypothesized that the second γH2AX peak may be associated with the G2/M mitotic arrest.

3.2. Mitotic phosphorylation of H2AX

Although it has been suggested that γH2AX is required for G2/M arrest induced by IR [24], the connection between γH2AX level and normal G2/M progression has not been well-documented. In addition, γH2AX has been reported during mitosis in the absence of DNA damage [11,21]. We hypothesized that the second peak of γH2AX at 8 h post-4 Gy irradiation could be due to the increased population of mitotic cells. We therefore synchronized the mitotic phase of HeLa cells using nocodazole and determined the change in γH2AX levels. As shown in Fig. 3A and B, the number of mitotic cells increased steadily and reached a peak at 16 h post-nocodazole (noc) treatment. Although there was no yield of DNA DSB after nocodazole treatment (Fig. 2C), the immunoblotting analysis showed that the level of γH2AX increased markedly in the synchronized mitotic cells, along with the appearance of the mitotic regulatory protein PLK1 (Fig. 3B). Consistent with this, the γH2AX level decreased sharply when the nocodazole block was removed (Fig. 3C). In addition, the level of the mitosis regulatory protein CCNB1 also declined, but declined relatively slowly. A portion of the cells exhibited γH2AX foci after nocodazole treatment for 16 h (Fig. 3D) and 24 h (Fig. 3E), and the percentage of the cells with more than 5 γH2AX foci per cell was shown in Fig. 3F. The abundant γH2AX foci were also demonstrated in some cells (red square box in Fig. 3D), which is consistent with a previous report [21].

3.3. DNA-PKcs contributes to the mitotic phosphorylation of H2AX

To identify the kinases contributing to the mitotic phosphorylation of H2AX, we used specific inhibitors targeting different PIKK family members. As shown in Fig. 4A, KU55933, a specific inhibitor of ATM, had little effect on the phosphorylation of H2AX in nocodazole-synchronized cells. However, the DNA-PKcs specific inhibitor NU7026 largely attenuated the H2AX phosphorylation (Fig. 4A, compare lane 4 with lane 2). The effect of NU7026 was further analyzed in the ATM-deficient cell lineAT5BIVA. The level of γH2AX also increased in AT5BIVA cells after nocodazole treatment, and this effect was inhibited by NU7026 (Fig. 4B). A decreased mitotic γH2AX induced by nocodazole was also observed in the DNA-PKcs depressed cells mediated by specific shRNA (Fig. 4C). Interestingly, we also observed a similar pattern of CHK2 Thr68 phosphorylation (Fig. 4C and D). Both KU55933 and NU7026 inhibited CHK2 phosphorylation (Fig. 4D), but inactivation of DNA-PKcs had a stronger effect than inactivation of ATM on CHK2 phosphorylation in mitotic cells. As shown in Fig. 4E, CHK2 phosphorylation is clearly induced by nocodazole in ATM-deficient AT5BIVA cells, and this effect is almost entirely eliminated by the DNA-PKcs inhibitor NU7026.

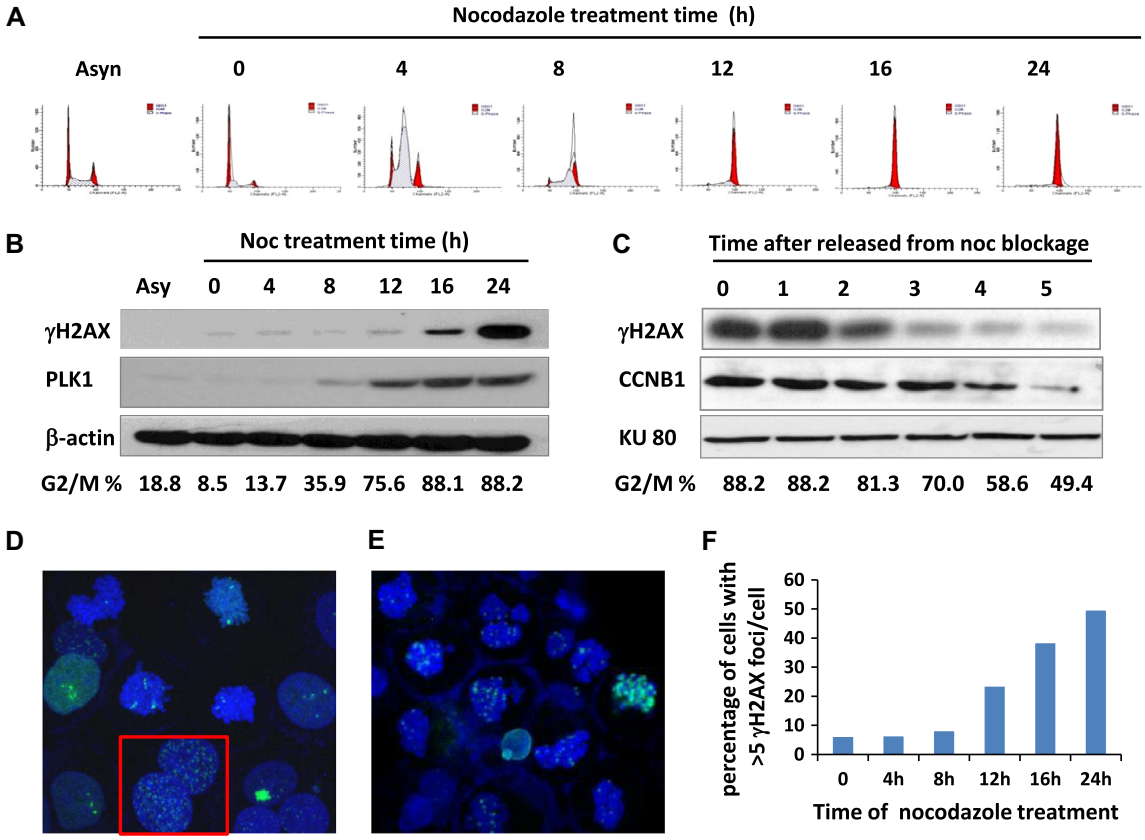

Fig. 3. Mitotic phosphorylation of H2AX. (A) The cell cycle distribution at the indicated time points after treatment with 100 ng/ml nocodazole. (B) γH2AX and PLK1 proteins were detected by immunoblotting analysis in the cells at the indicated time points post-nocodazole treatment. The proportion of G2/M cells populations was also given. (C) γH2AX and CCNB1 proteins detected by immunoblotting analysis in the cells at the indicated time points after releasing from the mitotic arrest. (D), (E) γH2AX foci formation was detected in cells mitotically arrested by treatment with 100 ng/ml nocodazole for 16 h and 24 h, respectively. (F) The percntage of cells with more than 5 γH2AX foci per cell after nocodazole treatment for 0–24 h.

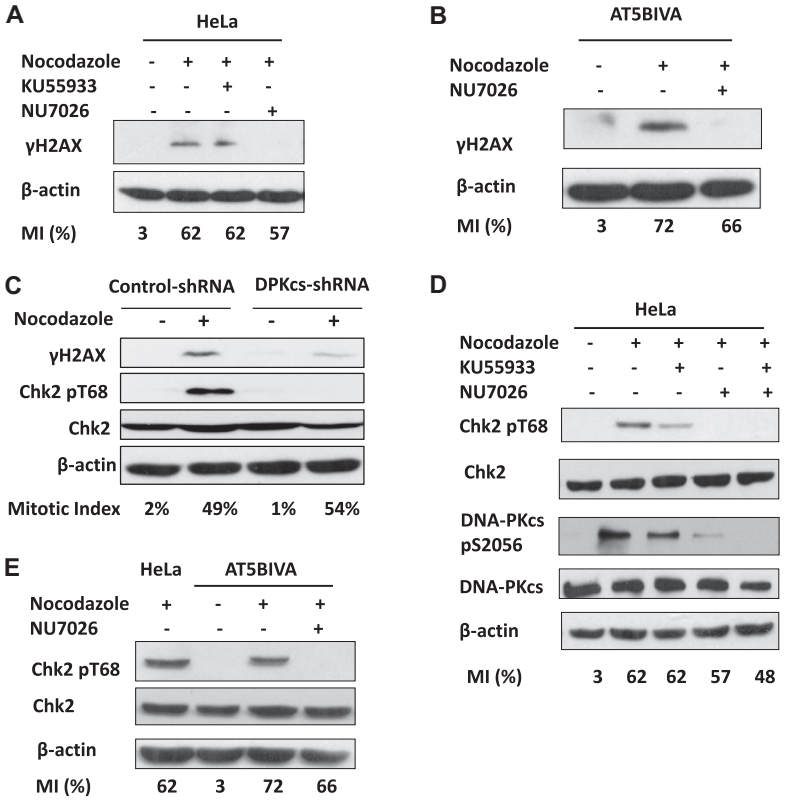

Fig. 4. DNA-PKcs regulates the mitotic phosphorylation of H2AX. (A, D) HeLa cells were treated with 100 ng/ml nocodazole for 14 h, and then DMSO (control) or NU7026 and/or KU55933 was added to the medium for another 2 h. Cells were collected for immunoblotting analysis of the indicated proteins. (B, E) ATM-deficient AT5BIVA cells were synchronized by nocodazole and treated with NU7026 or left untreated. γH2AX, CHK2, p-CHK2-T68 were detected by immunoblotting. (C) shRNA-mediated DNA-PKcs depleted HeLa cells (DPKcs-shRNA) and the control HeLa cells (control-shRNA) were synchronized by treated with nocodazole for 16 h or left untreated. γH2AX, p-CHK2-T68 were detected by immunoblotting.

3.4. CHK2-mediated H2AX phosphorylation during mitosis is regulated by DNA-PKcs

CHK2 is a substrate of both ATM and DNA-PKcs, and functions in cell cycle arrest upon DNA damage [25] as well as in normal mitosis progression [26]. We used an shRNA approach to generate a stable *Chk2* knock-down HeLa cell line (Fig. 5A). When CHK2 was depleted (HeLa$^{chk2\text{-}shRNA}$), we observed very low levels of γH2AX in synchronized mitotic cells (Fig. 5B). To further confirm this result, plasmids expressing an siRNA-resistant or an inactive form (T68A) of CHK2 were transfected into *chk2*-depleted HeLa$^{chk2\text{-}shRNA}$ cells. As shown in Fig. 5C, wild-type *chk2* effectively increased the γH2AX level, while the inactive form did not.

We did not detect γH2AX in asynchronized cells, and expression of either wild-type *chk2* or the phosphorylation-mimic chk2-T68D (active form) did not activate the H2AX phosphorylation in this population (Fig. 6, lane 1 to lane 3). As expected, an increase in γH2AX levels was detected in the nocodazole-synchronized cells, and this effect was largely attenuated by treatment with the DNA-PKcs inhibitor NU7026 (Fig. 6, lane 10), but not the ATM inhibitor NU55933 (Fig. 6, lane 7). Most importantly, the active phosphorylation-mimic *Chk2*-T68D (Fig. 6, lane 12), but not wild type *chk2* (*Chk2*-WT), (Fig. 6, lane 11) effectively abrogated the NU7026-mediated attenuation of mitotic γH2AX. This is most likely due to the fact that CHK2–WT could not be activated when DNA-PKcs was inactivated in the mitotic cells. CHK2-T68D also increased the γH2AX level in mitotic cells depleted of DNA-PKcs (data not shown). Together with the observation of DNA-PKcs phosphorylation (S2056) in mitotic cells (Fig. 4C), our results suggest that H2AX phosphorylation during mitosis is dependent on the DNA-PKcs / CHK2 pathway.

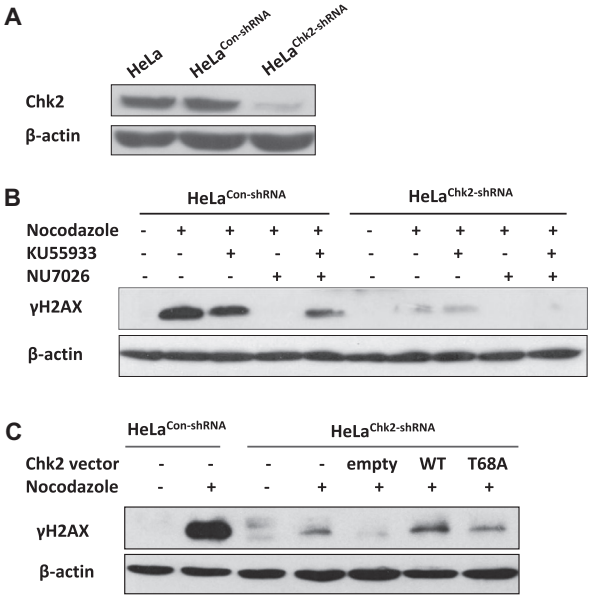

Fig. 5. CHK2 is essential for mitotic H2AX phosphorylation. (A) A stable *Chk2* knock-down HeLa cell line (HeLa$^{Chk2\text{-}shRNA}$) was generated by transfection with a *Chk2* shRNA expression vector and selection with hygromycin B. (B) Chk2-depleted HeLa cells and the control cells were synchronized with nocodazole and further treated with the DNA-PKcs inhibitor NU7026 and/or the ATM inhibitor NU55933. γH2AX was detected by immunoblotting. (C) Wild type or mutant (T68A) Chk2 was expressed in Chk2-depleted cells, and H2AX phosphorylation was detected by immunoblotting analysis.

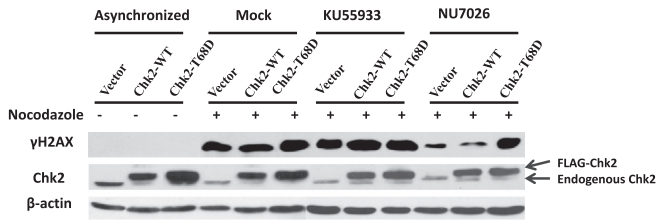

Fig. 6. The effect of CHK2-pT68 on the mitotic phosphorylation of H2AX, and regulation by PIKK family members. HeLa cells were transfected with empty vector or a plasmid expressing wild type *Chk2* or the phosphorylation mimic Chk2-T68D. At 36 h post transfection, the cells were synchronized with nocodazole for 14 h, then DMSO or 10 μM KU55933 or NU7026 was added to the medium for another 2 h, and the cells were collected for γH2AX detection by immunoblotting.

4. Discussion

The phosphorylation of H2AX at Ser139 is a critical event in the series of early responses to IR-induced DNA double-strand breaks [27]. Because of its early appearance and essential role in the DSB response, γH2AX is considered to be a sensitive biomarker for DSBs. In the present study, we demonstrate that H2AX phosphorylation also occurs during cell cycle progression, and that γH2AX levels increase when cells enter the M phase. The second peak in γH2AX levels after a high dose of irradiation could be attributed to the mitotic arrest. A similar observation was mentioned in a previous report [21], and it was suggested that this mitotic phosphorylation of H2AX was ATM-dependent. However, we have shown that DNA-PKcs, not ATM, is the major PIKK family kinase responsible for the mitotic phosphorylation of H2AX. KU55933, a specific chemical inhibitor of ATM, failed to inhibit H2AX phosphorylation in mitotic cells, while the DNA-PKcs specific inhibitor NU7026 significantly attenuated the mitotic γH2AX level. The decrease in mitotic γH2AX was further confirmed in DNA-PKcs knock-down cells.

Although DNA-PKcs was known to be involved in the mitotic phosphorylation of H2AX, it was unclear whether DNA-PKcs phosphorylates H2AX directly or through another kinase. Our results show that the cell cycle checkpoint protein CHK2 functions downstream of DNA-PKcs. Recently, CHK2 has also been reported to localize at centrosomes and play a role in normal mitotic progression through regulating the assembly of the spindle [23,26,28]. Here we show that CHK2 is phosphorylated at Thr68 in a DNA-PKcs-dependent manner during normal cell cycle progression, and has a similar phosphorylation pattern as γH2AX in mitotic cells. These results are consistent with a recent report that showed that CHK2 phosphorylation in response to IR is impaired in cells with a defective DNA-PKcs, or in the presence of a DNA-PKcs inhibitor in certain cell lines [29].

Silencing CHK2 significantly impacts the mitotic phosphorylation of H2AX. The role of CHK2 was further confirmed using mutants that prevent (T68A) or mimic (T68D) Thr68 phosphorylation. The phosphorylation-mimic CHK2-T68D abrogated the repression of H2AX phosphorylation by NU7026, and overexpression of WT, but not T68A, in a stable CHK2 knockdown cell line increases γH2AX levels post-nocodazole treatment. Taken together, these data demonstrate an essential role for CHK2 in mediating the mitotic phosphorylation of H2AX.

In mammalian cells, H2AX phosphorylation is regulated by multiple pathways (Fig. 7), including phosphorylation by PIKK family kinases and dephosphorylation by protein phosphatases including PP2A, PP4, PP6 and WIP1. Protein phosphatase 2A (PP2A) was the first γH2AX dephosphorylating agent to be identified [30,31], and inhibition or silencing of PP2A leads to γH2AX foci persistence and defects in DNA repair. PP2A is a member of a family of protein phosphatases composed of multiple catalytic subunits and regulatory subunits [31]. B56, the regulatory B subunit of PP2A, is directly phosphorylated by ATM, generating B56γ3, B56γ2 and B56δ, which results in the formation of the B56γ3-PP2A complex [32]. Inhibition of ATM by KU55933 could result

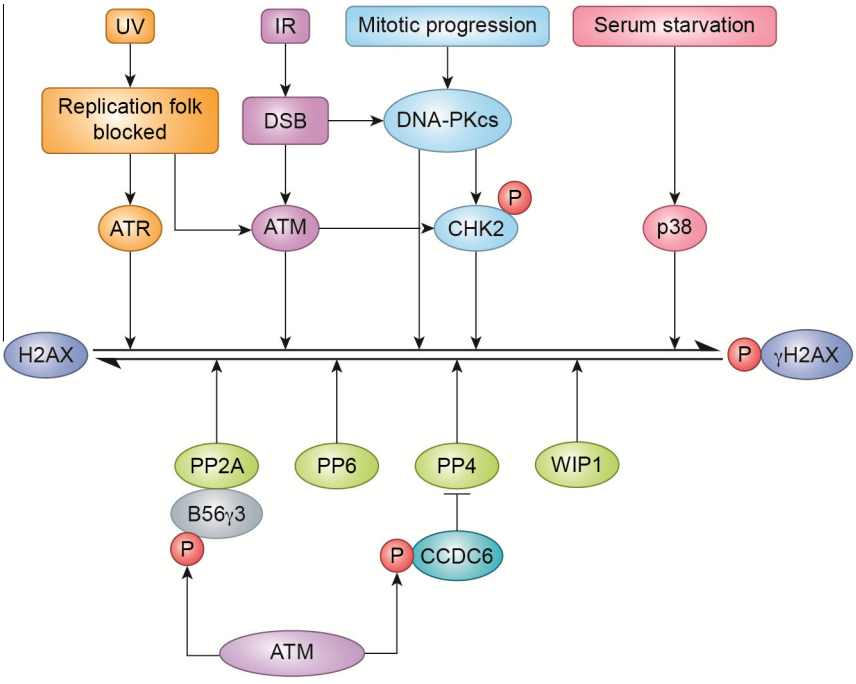

Fig. 7. Schematic showing the regulation of H2AX phosphorylation and dephosphorylation. In response to UV radiation-induced replication folk blockage (RFB), ATR and/or ATM is activated, resulting in the phosphorylation of H2AX. Upon DSB induction by ionizing radiation, both the activated ATM and DNA-PKcs mediate H2AX phosphorylation. During mitotic progression, DNA-PKcs is activated and activates CHK2, which in turn mediates H2AX phosphorylation. Serum starvation induces the phosphorylation of H2AX through the p38 MAPK signaling pathway. Multiple protein phosphatases mediate the dephosphorylation of γH2AX, which may also be regulated by the PIKK family members.

in decreased dephosphorylation by PP2A, which may partially offset its effect of phosphorylating H2AX. However, this would be a very complex regulatory system for the protein phosphatases. PP4 is another protein phosphatase that dephosphorylates γH2AX and is implicated in DNA damage response [31,33,34]. A recent report indicated that the coiled coil domain-containing 6 (CCDC6) protein can interact with and negatively regulate the activity of the catalytic subunit of PP4 (PP4c). Depletion of CCDC6 decreased γH2AX levels due to an accelerated rate of dephosphorylation [35]. ATM mediates the phosphorylation of CCDC6 at Thr434, which inhibits the FBXW6-CCDC6 interaction and FBXW7-mediated CCDC6 degradation [36]. Therefore, the PIKK family members could exert a composite regulatory effect on the activity of protein phosphatase family members.

In conclusion, we report the cell cycle-dependent phosphorylation of H2AX in the absence of DNA damage and show that DNA-PKcs and CHK2 are two important kinases involved in this process (Fig. 7). Activated CHK2 directly mediates the mitotic phosphorylation of H2AX. Based on our results, we suggest that studies using γH2AX as a biomarker for the repair kinetics of IR-induced DNA DSBs should be interpreted with caution.

5. Conflict of Interest

None declared.

Acknowledgements

This work was supported by the National High Technology Research and Development Program of China (863 Program, Grant number: 2012AA063501), the Chinese National Natural Science Foundation (Grant number: 81071678 and 81272994) and the Lotus Scholars Program of Hunan Provincial People's Government.

Appendix A. Supplementary data

Supplementary data associated with this article can be found, in the online version, at http://dx.doi.org/10.1016/j.febslet.2013.08.028.

References

[1] Zhou, P. (2011) DNA damage, signaling and repair: Protecting genomic integrity and reducing the risk of human disease. Chinese Sci. Bull. 56, 3119–3121.
[2] Scott, S.P. and Pandita, T.K. (2006) The cellular control of DNA double-strand breaks. J. Cell Biochem. 99, 1463–1475.
[3] Hunt, C.R., Ramnarain, D., Horikoshi, N., Iyenger, P., Pandita, R.K., Shay, J.W. and Pandita, T.K. (2013) Histone Modifications and DNA Double-Strand Break Repair after Exposure to Ionizing Radiations. Radiat. Res. 179, 383–392.
[4] Rogakou, E.P., Pilch, D.R., Orr, A.H., Ivanova, V.S. and Bonner, W.M. (1998) DNA double-stranded breaks induce histone H2AX phosphorylation on serine 139. J. Biol. Chem. 273, 5858–5868.
[5] West, M.H. and Bonner, W.M. (1980) Histone 2A, a heteromorphous family of eight protein species. Biochemistry 19, 3238–3245.
[6] Foster, E.R. and Downs, J.A. (2005) Histone H2A phosphorylation in DNA double-strand break repair. FEBS J. 272, 3231–3240.
[7] Paull, T.T., Rogakou, E.P., Yamazaki, V., Kirchgessner, C.U., Gellert, M. and Bonner, W.M. (2000) A critical role for histone H2AX in recruitment of repair factors to nuclear foci after DNA damage. Curr. Biol. 10, 886–895.
[8] Stucki, M. and Jackson, S.P. (2006) GammaH2AX and MDC1: anchoring the DNA-damage-response machinery to broken chromosomes. DNA Repair (Amst) 5, 534–543.
[9] Yuan, J., Adamski, R. and Chen, J. (2010) Focus on histone variant H2AX: to be or not to be. FEBS Lett. 584, 3717–3724.
[10] Celeste, A. et al. (2002) Genomic instability in mice lacking histone H2AX. Science 296, 922–927.
[11] An, J. et al. (2010) DNA-PKcs plays a dominant role in the regulation of H2AX phosphorylation in response to DNA damage and cell cycle progression. BMC Mol. Biol. 11, 18.
[12] Burma, S., Chen, B.P., Murphy, M., Kurimasa, A. and Chen, D.J. (2001) ATM phosphorylates histone H2AX in response to DNA double-strand breaks. J. Biol. Chem. 276, 42462–42467.
[13] Ward, I.M., Minn, K. and Chen, J. (2004) UV-induced ataxia-telangiectasia-mutated and Rad3-related (ATR) activation requires replication stress. J. Biol. Chem. 279, 9677–9680.
[14] Wang, H., Wang, M., Wang, H., Bocker, W. and Iliakis, G. (2005) Complex H2AX phosphorylation patterns by multiple kinases including ATM and DNA-PK in human cells exposed to ionizing radiation and treated with kinase inhibitors. J. Cell Physiol. 202, 492–502.
[15] Kobayashi, J., Antoccia, A., Tauchi, H., Matsuura, S. and Komatsu, K. (2004) NBS1 and its functional role in the DNA damage response. DNA Repair (Amst) 3, 855–861.
[16] Keogh, M.C. et al. (2006) A phosphatase complex that dephosphorylates gammaH2AX regulates DNA damage checkpoint recovery. Nature 439, 497–501.
[17] Valdiglesias, V., Giunta, S., Fenech, M., Neri, M. and Bonassi, S. (2013) GammaH2AX as a marker of DNA double strand breaks and genomic instability in human population studies. Mutat. Res. 753, 24–40.
[18] Cleaver, J.E., Feeney, L. and Revet, I. (2011) Phosphorylated H2Ax is not an unambiguous marker for DNA double-strand breaks. Cell Cycle 10, 3223–3224.
[19] Revet, I., Feeney, L., Bruguera, S., Wilson, W., Dong, T.K., Oh, D.H., Dankort, D. and Cleaver, J.E. (2011) Functional relevance of the histone gammaH2Ax in the response to DNA damaging agents. Proc. Natl. Acad. Sci. USA 108, 8663–8667.
[20] Lu, C., Shi, Y., Wang, Z., Song, Z., Zhu, M., Cai, Q. and Chen, T. (2008) Serum starvation induces H2AX phosphorylation to regulate apoptosis via p38 MAPK pathway. FEBS Lett. 582, 2703–2708.
[21] McManus, K.J. and Hendzel, M.J. (2005) ATM-dependent DNA damage-independent mitotic phosphorylation of H2AX in normally growing mammalian cells. Mol. Biol. Cell 16, 5013–5025.
[22] Shang, Z.F. et al. (2012) 4E-BP1 participates in maintaining spindle integrity and genomic stability via interacting with PLK1. Cell Cycle 11, 3463–3471.
[23] Stolz, A. et al. (2010) The CHK2-BRCA1 tumour suppressor pathway ensures chromosomal stability in human somatic cells. Nat. Cell Biol. 12, 492–499.
[24] Fernandez-Capetillo, O. et al. (2002) DNA damage-induced G2-M checkpoint activation by histone H2AX and 53BP1. Nat. Cell Biol. 4, 993–997.
[25] Canton, D.A. and Scott, J.D. (2010) Chk-ing in and Chk-ing out: kinase compartmentalization comes to checkpoint control. Mol. Cell 40, 1–2.
[26] Tsvetkov, L., Xu, X., Li, J. and Stern, D.F. (2003) Polo-like kinase 1 and Chk2 interact and co-localize to centrosomes and the midbody. J. Biol. Chem. 278, 8468–8475.
[27] Fillingham, J., Keogh, M.C. and Krogan, N.J. (2006) GammaH2AX and its role in DNA double-strand break repair. Biochem. Cell Biol. 84, 568–577.
[28] Chouinard, G., Clement, I., Lafontaine, J., Rodier, F. and Schmitt, E. (2013) Cell cycle-dependent localization of CHK2 at centrosomes during mitosis. Cell Div. 8, 7.
[29] Li, J. and Stern, D.F. (2005) Regulation of CHK2 by DNA-dependent protein kinase. J. Biol. Chem. 280, 12041–12050.
[30] Chowdhury, D., Keogh, M.C., Ishii, H., Peterson, C.L., Buratowski, S. and Lieberman, J. (2005) Gamma-H2AX dephosphorylation by protein phosphatase 2A facilitates DNA double-strand break repair. Mol. Cell 20, 801–809.
[31] Liu, B. and Xu, X.-Z. (2011) Serine/threonine protein phosphatases in DNA damage response. Chinese Sci. Bull. 56, 3122–3131.
[32] Shouse, G.P., Nobumori, Y., Panowicz, M.J. and Liu, X. (2011) ATM-mediated phosphorylation activates the tumor-suppressive function of B56gamma-PP2A. Oncogene 30, 3755–3765.
[33] Nakada, S., Chen, G.I., Gingras, A.C. and Durocher, D. (2008) PP4 is a gamma H2AX phosphatase required for recovery from the DNA damage checkpoint. EMBO Rep. 9, 1019–1026.
[34] Chowdhury, D. et al. (2008) A PP4-phosphatase complex dephosphorylates gamma-H2AX generated during DNA replication. Mol. Cell 31, 33–46.
[35] Merolla, F., Luise, C., Muller, M.T., Pacelli, R., Fusco, A. and Celetti, A. (2012) Loss of CCDC6, the first identified RET partner gene, affects pH2AX S139 levels and accelerates mitotic entry upon DNA damage. PLoS One 7, e36177.
[36] Zhao, J., Tang, J., Men, W. and Ren, K. (2012) FBXW7-mediated degradation of CCDC6 is impaired by ATM during DNA damage response in lung cancer cells. FEBS Lett. 586, 4257–4263.